Saudi Pharmaceutical Journal 28 (2020) 927–935

Contents lists available at ScienceDirect

Saudi Pharmaceutical Journal

journal homepage: www.sciencedirect.com

Original article

Formulation and optimization of quinoa starch nanoparticles: Quality by design approach for solubility enhancement of piroxicam

Meenakshi Bhatia *,[1], Sulekha Rohilla

Guru Jambheshwar University of Science and Technology, Hisar 125 001, India

ARTICLE INFO

Article history:
Received 2 March 2020
Accepted 20 June 2020
Available online 24 June 2020

Keywords:
Quinoa starch
Piroxicam
Nanoprecipitation
Anti-oxidant
In-vitro anti-inflammatory
Solubility enhancement

ABSTRACT

In the present study piroxicam loaded starch nanoparticles were prepared to enhance the solubility of piroxicam by nanoprecipitation technique. The preparation of nanoparticles was carried out as per central composite experimental design protocol, having concentration of starch and drug as independent variables and particle size and polydispersity index (PdI) as dependent variables. The particle size and PdI of piroxicam loaded starch nanoparticles was found to be between 282–870 nm and 0.339–0.772, respectively. After the characterization by FT-IR, TGA, XRD and SEM studies, the optimized batch was evaluated for in-vitro release study, anti-inflammatory activity and anti-oxidant activity. The in-vitro anti-inflammatory activity of piroxicam loaded starch nanoparticles was found to be more than the pure drug piroxicam whereas the anti-oxidant activity of starch is found greater than starch nanoparticles. In-vitro release study showed 98.8% release in 2 h dissolution study following supercase II transport mechanism of drug release.

1. Introduction

Starch, glycogen and cellulose are three most abundant organic homopolymers found in nature. Starch is a polymeric carbohydrate that consists of large number of glucose units joined by α-1, 4 glycosidic linkages having a basic chemical formula as $(C_6H_{10}O_5)_n$. It may consist of 20–30% amylose, a linear polysaccharide and 70–80% amylopectin, a branched polysaccharide (Wang and Copeland, 2015). It is stored in chloroplasts in the form of granules, in roots of tapioca plant, in tuber of potato, in stem pith of sago and seeds of corn, wheat, chest nuts and rice etc. Besides its nutritional values or uses, starches are used in paper, textile, brewing, adhesive, bakery, food and pharmaceutical industry. Starch obtained from different sources has gained attention of researchers for various applications in pharmaceutical field viz. corn starch utilized for making bio-based films implemented in food (Araújo et al., 2018), water chestnut starch for encapsulation of probiotic bacterial cells (Ahmad et al., 2019) tapioca and potato starch employed to produce the bionanocomposite films (Gopi et al., 2019), wheat starch used to manufacture biodegradable nanoporous aerogels (Ubeyitogullari and Ciftci, 2016), horse chestnut (HSC), water chestnut (WSC) and lotus stem (LSC) starch for nano-encapsulation of catechin (Ahmad et al., 2019a, 2019b) , waxy maize starch utilized to prepare the nanocrystals aqueous suspensions (Angellier et al., 2004), quinoa starch stabilizing particles for production of pickering emulsions (Rayner et al., 2012), sweet potato starch as microparticles for production of controlled drug release applications (Liu et al., 2007), rice starch as thin films intended for buccal delivery systems (Chan et al., 2019) and so on.

Natural polysaccharide like alginate, starch, dextran, cellulose, psyllium, flaxeed, xanthan gum, chitosan, etc. provides a feasible substitute to the conventional non-biodegradable polymers (Farrag et al., 2018; Ahuja et al., 2016; Bhatia and Saini, 2018; Bhatia and Ahuja, 2013; Devi and Bhatia, 2019; Bhatia et al., 2015). Natural polysachharides and starches possess several advantages like easy availability, biodegradability, excellent biocompatibility, decreased toxicity and side effects etc. These properties render them as a suitable and potential carrier in drug delivery systems.

The quinoa starch is obtained from the seeds of the plant *chenopodium quinoa* belonging to the family *chenopodiaceae*. The seeds of quinoa composed of high content of proteins and vital free amino

* Corresponding author.
E-mail address: meenaxibhatia@gmail.com (M. Bhatia).
[1] Drug Delivery Research Laboratory, Department of Pharmaceutical Sciences, Guru Jambheshwar University of Science and Technology, Hisar 125 001, India.

Peer review under responsibility of King Saud University.

Production and hosting by Elsevier

https://doi.org/10.1016/j.jsps.2020.06.013
1319-0164/

acids in a balanced manner, various vitamins in small concentration, starch, oils, minerals and anti-oxidants etc. (Letelier et al., 2011; Sezgin and Sanlier, 2019) . Quinoa is also known for its incredible amounts of phytochemicals like flavonoids, phytosterols, polyphenols and saponins (D'Amico et al., 2019). Seeds of quinoa have bagged popularity due to high nutritive value and its vast pharmaceutical applications render it a suitable candidate to be explored for more applications in the field (Stikic et al., 2012). From past few years, nanoparticles acquired from biodegradable sources have awakened very much awareness.

The traditional methods for the preparation of starch nanoparticles accommodate nanoprecipitation, self-assembly, emulsification, acid hydrolysis, solvent evaporation, monomer polymerization, salting out, emulsification- solvent evaporation, extrusion high pressure homogenization, supercritical fluid extraction, emulsion crosslinking, emulsion solvent diffusion, ethanol injection and ionic gelation and ball milling etc. (Farrag et al., 2018; Liu et al., 2018; Govender et al., 1999; Ding et al., 2019; Qin et al., 2016; El-Sheikh, 2017; Rivas et al., 2017; Ahmad et al., 2020) . Out of these techniques, the extremely simple and reproducible technique for the nanoparticles preparation tends to be nanoprecipitation that has been extensively employed in past viz. microfluidic nanoprecipitation for delivery of anti viral drugs (Bramosanti et al., 2017), two step nanoprecipitation for enhanced drug loading capacity of 10-hydroxycamptothecin-loaded (Wang and Tan, 2016), solvent-nonsolvent nanoprecipitation technique for preparing curcumin nanoparticles (Khan and Rathod, 2014), bottom up nanoprecipitation technique for the formation of hydrocortisone nanosuspension (Ali et al., 2009), controlled nanoprecipitation method without surfactants for the delivery of cefroxime (Zhang et al., 2006) and flash nanoprecipitation (Fu et al., 2019) etc.

The drug piroxicam is a dynamic NSAID belongs to BCS-II is described as practically insoluble in water (0.023 mg/ml) and is widely employed in the treatment of acute and chronic musculoskeletal and joint disorders such as rheumatoid arthritis, osteoarthritis, ankylosing spondylitis (Adebisi et al., 2016; Gholivand et al., 2014) , is used as a model drug in this piece of research. The mode of action of NSAIDs includes the inhibition of the enzyme cyclooxygenase (COX) which is responsible for the cause of inflammation (Legrand, 2004).

In the present study, preparation of piroxicam loaded quinoa starch nanoparticles is described. Because of absence of gluten and its consideration as sacred herb, quinoa starch is prospected as a carrier in this piece of research for its applications in enhancing the solubility of BCS II drug. The simple and reproducible technique of nanoprecipitation was utilized for preparing piroxicam loaded starch nanoparticles with the objective to improve the solubility of drug. The preparation was carried out as per the design protocol as suggested by the 2-factor, 3-level central composite experimental design (Design Expert software version 7.16). The optimized batch was characterized by FT-IR, TGA, XRD and SEM. The average particle size and polydispersity index was determined by using zetasizer. The optimized batch was further evaluated for *in-vitro* anti-oxidant activity, anti-inflammatory activity and release kinetics.

2. Experimental

2.1. Materials and methods

Quinoa seeds were purchased from the Organic India Pvt. Ltd. (Uttar Pradesh, India). Sodium hydoxide and DPPH (2,2-Diphenyl-1-Picryl Hydrazyl) were purchased from High Purity Laboratory chemicals Pvt. Ltd. Piroxicam drug was purchased from HiMedia Laboratories Pvt. Ltd. All other chemicals like Ethanol, Glycerol, HCl (SD Fine Chemical Ltd., India) used in this study were of analytical grade and utilized as received.

2.2. Isolation of starch

The starch from the seeds of quinoa was extracted through the water-steeping method (Jan et al., 2017) with slight modification. In this method, the seeds of quinoa were crushed and then soaked in water (1:6) for 24 h, succeeded by wet milling for about 10 min through a mechanical stirrer. The obtained slurry was then filtered through the succession of BSS sieves (100, 200 and 300 mesh size). The procured filtrate was then centrifuged at 5000 rpm for 15 min. and the supernatant was discarded away. The starch cake retrieved was again suspended in the water and centrifuged for 10 min. The drying process of purified starch cake was done in the hot air oven at 40 °C till constant weight and then stored in desiccator for further use.

2.3. Preparation of starch nanoparticles

According to the method reported, starch nanoparticles (SNPs) were prepared by means of nanoprecipitation technique (Farrag et al., 2018) with certain changes. In the present study, starch (5–10 mg/ml) was dispersed in solvent system of NaOH, glycerin and distilled water in the ratio of (0.8:1:98.2 w/w) (El-Sheikh, 2017). The dispersion was prepared by using the magnetic stirrer at an rpm of 1000–2000. The process of mixing was continued for 30 min and then mixture was kept undisturbed for 2 h at room temperature for equilibration. For nanoprecipitation, 10 ml of starch solution was placed in a 100 ml beaker and then 25 ml of 0.1 M HCl was added dropwise under continuous stirring at 1000 rpm. The produced particles were centrifuged at 5000 rpm for 10 min. and then were washed with 35% aqueous ethanol followed by washing with distilled water. The nanoparticles were then freezed at −80 °C and lyophilized in a laboratory lyophiliser (Alpha 2–4 LD Plus Germany) at a pressure of 0.2 mbar for 24 h.

2.4. Preparation of starch-piroxicam nanoparticles

The starch-piroxicam nanoparticles were prepared by following the similar procedure as described above, employing nanoprecipitation technique. Design Expert Software (version 7.16) was used for the preparation and optimization of PSNPs accepting 2-factor, 3-level central composite experimental design. Piroxicam (2.5–10 mg/ml) was added to the NaoH/glycerin/H_2O solution containing the 5–10 mg/ml concentration of starch (Table 1). The process of adding 0.1 M HCl solution was maintained at a constant rate. The produced particles were centrifuged at 5000 rpm for 10 min. and then washed with 35% ethanol and distilled water. The nanoparticles were then freezed at −80 °C and lyophilized at 0.2 mbar for 24 h.

2.5. Experimental design

Various batches of starch-piroxicam nanoparticles were prepared and optimized using a 2-factor, 3-level central composite experimental design (Table 1). The formulation variables include conc. of starch (X_1) and conc. of drug (X_2) whereas selected response variables were particle size or z-avg (d.nm) (Y_1) and polydispersity index (PdI) (Y_2). Every independent variable was examined at 3levels viz. (−1, 0, +1). The statistical analysis and experimental design was carried out using Software Design Expert (version 7.16).

Table 1
z-average and polydispersity index of different batches of piroxicam loaded starch nanoparticles.

Batch	conc. of starch (mg/ml) (X_1)	conc. of piroxicam (mg/ml) (X_2)	z-avg. (d.nm) (Y_1)	Polydispersity index (PdI) (Y_2)
1	5	6.25	746	0.691
2	10	10	291	0.339
3	7.5	6.25	406.8	0.478
4	7.5	6.25	409.4	0.457
5	7.5	6.25	437	0.546
6	10	2.5	332.6	0.422
7	7.5	10	320.9	0.415
8	10	6.25	438.3	0.453
9	7.5	2.5	282.9	0.379
10	7.5	6.25	494	0.503
11	5	10	870.5	0.772
12	7.5	6.25	369.7	0.455
13	5	2.5	406	0.444

2.6. Characterization

2.6.1. Fourier transform infra-red spectroscopy (FT-IR)

The FT-IR spectra of the Starch, Piroxicam and PSNPs were examined in the wavelength range of 4000–500 cm^{-1} using Fourier transform infra-red spectroscopy (Perkin-Elmer, Spectrum) using KBr pellet method.

2.6.2. Thermal analysis

Thermal behavior and differential scanning calorimetery (DSC) of Starch, Piroxicam and PSNPs was studied by using a simultaneous thermal analyzer (SDT, Q600, TA instruments, USA) at a temperature range from 0 to 310 °C at a heating rate of 10 °C/min under the constant purge of nitrogen.

2.6.3. Powder X-ray diffraction (PXRD) analysis

PXRD pattern of Starch, Piroxicam, and PSNPs were scanned using X-ray diffractometer (Miniflex 2, Rigaku, Japan) from 10° to 80° diffraction angle (2θ) range. X-ray diffractometer was operated at 30 kV and 15 mA with a nickel filtered Cu-Kα radiation. The speed of scanning was 0.05 min^{-1} with the division slit 1.25° and receiving slit 0.3 mm.

2.7. Scanning electron microscopy (SEM)

The shape and surface morphology of optimized formulation was examined through scanning electron microscope (JSM-6100, Scanning microscopy, Japan). The sample was coated with gold and mounted on the stubs.

2.8. Particle size analysis

The average particle size and polydispersity index of the formulations were determined by using Zetasizer (Nano ZS 90, Malvern Instruments, UK) at a temperature of 25 °C. The measurements were performed in an automated mode.

2.9. Evaluation of piroxicam starch nanoparticles (PSNPs)

2.9.1. Entrapment efficiency and drug loading

The dried PSNPs procured from the earlier explained method were weighed. The nanoparticles (5 mg) was dispersed in the NaOH/glycerin/H_2O solution. The absorbance in the solution was determined instantly through a *uv–vis.* Spectrophotometer (Varian Cary 5000, Australia) at λ_{max} of 354 nm. The calibration curve of piroxicam was prepared in the NaOH/glycerin/ H_2O solution. After suitable dilutions of dispersed PSNPs, the absorbance was measured and then compared with the corresponding calibration curve. The drug loading and entrapment efficiency were calculated using Eqs. (1) and (2) (Farrag et al., 2018; Papadimitriou and Bikiaris, 2009) .

$$\textit{Drug loading}\ (\%) = \frac{\textit{weight of drug in nanoparticles}}{\textit{weight of nanoparticles}} \times 100 \quad (1)$$

$$\textit{Entapment efficiency}\ (\%) = \frac{\textit{weight of drug in nanoparticles}}{\textit{weight of drug fed initially}} \times 100 \quad (2)$$

2.10. DPPH radical scavenging activity

The anti-oxidant activity of quinoa starch and blank starch nanoparticles was determined by using 1,1-Diphenyl-2-picrylhydrazyl (DPPH) assay method (Xu et al., 2019) with slight modification. Different concentrations (0.4, 0.8, 1.2, 1.6 and 2.0 mg/ml) of starch were prepared by mixing it with a solution of NaOH/glycerin/H_2O. After this, 2.0 ml of above starch solution of each concentration was added to the 3 ml of 0.1 mM freshly prepared DPPH-ethanol solution and then permitted to react for 30 min. The absorbance of all solutions of different concentrations was measured at a wavelength of 517 nm (A_1). For blank/control, ethanol was used and the absorbance measured was named as A_0. To measure the absorbance A_2, DPPH solution was replaced by the NaOH/glycerin/H_2O solution. The anti-oxidant activity of blank SNP was measured using the above mentioned method. DPPH radical scavenging activity (%) was calculated by the following given Eq. (3) as under:-

$$\textit{DPPH radical scavenging activity}\ (\%) = (A_0 - A_1 + A_2)/A_0 \times 100 \quad (3)$$

2.11. Anti-inflammatory activity

The *in-vitro* anti-inflammatory activity of model drug piroxicam and PSNPs were estimated by using the egg albumin denaturation method with slight modification (Chavan and Hosamani, 2018). The mixture was composed of 0.2 ml of fresh hen egg's albumin, 2.8 ml of PBS (Phosphate buffered saline, pH 6.4) and 2 ml of different concentrations of PSNPs (125, 250, 500 and 1000 μg/ml) in DMSO. The mixtures so obtained were placed in an incubator (Caltan, NSW, India) at a temp of 37 ± 2 °C for 15 min incubation followed by heating at 70 °C. Further, the mixtures were allowed to cool at room temp and absorbance was measured at a wavelength of 660 nm. Similar experiment was performed for the model drug piroxicam with the same concentrations as taken for the formulation as a reference or control. The following given Eq. (4) was employed for calculating the % inhibition of protein denaturation.

$$\%\ \text{Inhibition} = 100 \times \frac{\text{Abs of control} - \text{Abs of sample}}{\text{Abs of control}} \quad (4)$$

2.12. In-vitro drug release study

The in-vitro release profile of piroxicam from the optimized batch of nanoparticles and pure drug solution was carried out using dialysis bag diffusion technique (Gandhi et al., 2014). An accurately weighed amount of drug loaded nanoparticles containing drug equivalent to 20 mg piroxicam and pure drug (20 mg) were placed in the dialysis tubing (cut off 10,000 kDa) containing 5 ml of 0.1 N HCl. The hermetically sealed dialysis tubing was then tied to the paddle of USP type II dissolution apparatus (TDL-08L, Electro lab, India) and then immersed into the 250 ml of 0.1 N HCl as dissolution media maintained at 37 ± 1 °C at 100 rpm. Samples (5 ml) were withdrawn using the pipette at regular time intervals for 120 min. and replaced with same amount of fresh dissolution media to maintain the sink condition during the experiment. The absorbance of the samples was measured at the wavelength of 242 nm to determine the concentration of piroxicam in the samples using the *uv–vis* spectrophotometer. The experiment was performed in the triplicate. Further, the release data was fitted in different release kinetics models to determine the mechanism of drug release.

3. Result and discussion

3.1. Fourier transform infra-red spectroscopy (FT-IR)

FT-IR is a beneficial tool for the identification of drugs and samples. Fig. 1 (a, b and c) exhibits the FT-IR spectra of starch, Piroxicam and piroxicam loaded starch nanoparticles (PSNPs) respectively in the frequency range of 4000–400 cm^{-1}. The spectrum of starch shows a broad absorption band at the 3409.22 cm^{-1} which may be due to –OH stretching of alcohol. The absorption band at 2932.06 cm^{-1} and 1329.94 cm^{-1} may be attributed to —CH stretching of alkane and —OH bending of alcohol, respectively. The peak appearing at 1041.41 cm^{-1} may be due to —CO stretching of primary amine. The IR spectra spectrum of piroxicam shows the characteristic peak at 3393.60 cm^{-1} that may be ascribed to —OH stretching of alcohol while peaks appearing at 3337.92 cm^{-1} and 3067.86 cm^{-1} can be ascribed to –NH stretching of secondary amine and —CH stretching of alkanes, respectively. The peaks appearing at 1630.08 cm^{-1}, 1435.61 cm^{-1} and 1150.69 cm^{-1} can be due to —C=O stretching of secondary amide, —CH bending of alkane and —CN stretching of amine, respectively. The peaks appearing at 1039.31 cm^{-1} and 774.95 cm^{-1} may be due to —SO_2 stretching and —CH bending monosubstituted, respectively. The IR spectrum of piroxicam loaded starch nanoparticles exhibits a broad absorption band at 3437.21 cm^{-1} instead of sharp peaks at 3393.60 cm^{-1} that are seen in FTIR spectra of drug, which may be attributed to —OH stretching of alcohol while peaks appearing at 1638.48 cm^{-1} and 1399.25 cm^{-1} may be due to —C=O stretching of secondary amide and —OH bending of alcohol, respectively. The peaks at 1159.59 cm^{-1} and 1027.72 cm^{-1} shows presence of —CN stretching of amine and —CO stretching of primary alcohol, respectively. The peak appearing at 769.90 cm^{-1} can be ascribed to —CH bending monosubstitute. The spectrum of piroxicam loaded starch nanoparticles demonstrated a slight shift of the peak at 3437.21 cm^{-1} due to interaction between drug piroxicam and starch as a carrier that confirms the successful formation of nanoparticles and also the entrapment of drug.

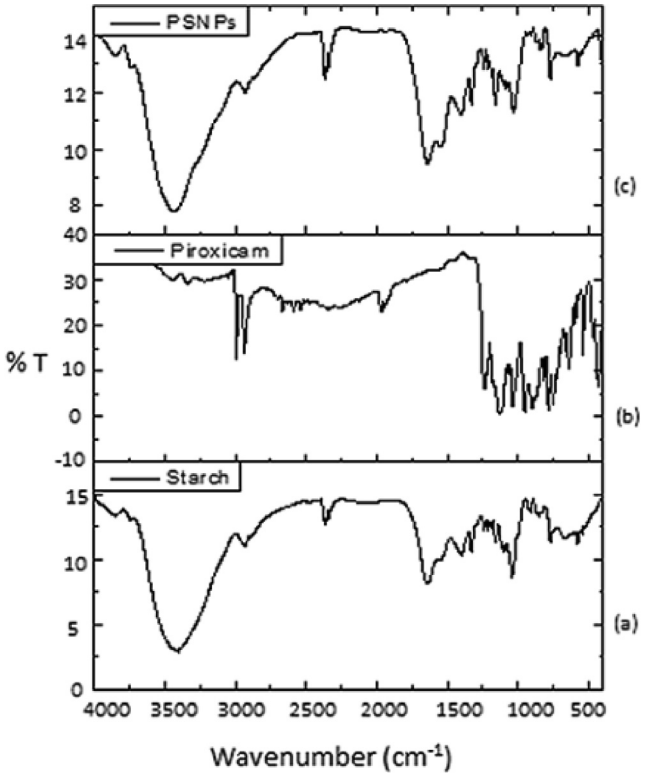

Fig. 1. FT-IR spectra of (a) Starch (b) Piroxicam and (c) PSNPs.

3.2. Thermal analysis

Fig. 2 (a, b and c) displays the differential scanning calorimetery, first derivative and DTG curves of isolated starch, piroxicam and PSNPs, respectively. There is no sharp peak in thermogram of starch i.e. typical of amorphous material. The thermogram of piroxicam exhibits an endotherm at 202 °C that corresponds to its melting point whereas the DSC studies of PSNPs displays the crystalline nature of the product. Thermal analysis provide indication about physical nature and also the thermal stability of the samples. The first derivative and DTG curves exhibit the sail of weight loss with increasing temperature w.r.t. starch, piroxicam and PSNPs. Starch being amorphous shows an initial weight loss drip or decomposition at around 100 °C whereas drug piroxicam and PSNPs are showing weight loss at around 200 °C (Fig. 2b) display stability of the product at higher temperature.

3.3. X-ray diffraction (XRD) analysis

Fig. 3 demonstrated the XRD patterns of starch, piroxicam and PSNPs. The diffractogram of starch is of amorphous material having peaks of less intensity at 14.86°, 16.64°, 22.64° and 22.90° at diffraction angle (2θ). The x-ray diffractogram of piroxicam shows the characteristic peaks at 14.48°, 17.64°, 17.68°, 17.70°, 27.32°, 27.38° and 27.42° that is typical of crystalline nature whereas XRD pattern of PSNPs shows that PSNPs possess the properties of both type of nature i.e. of amorphous and crystalline with some degree of reflectivity too, thus indicating a change has occurred. Hence, it is inferred from the plot that nanoprecipitation has imparted the amorphous character.

3.4. Scanning electron microscopy

Fig. 4 shows the surface morphology of the optimized batch of Piroxicam loaded starch nanoparticles (PSNPs) which are investigated under the scanning electron microscope. The results demonstrated PSNPs with flaky, rough and granular surface.

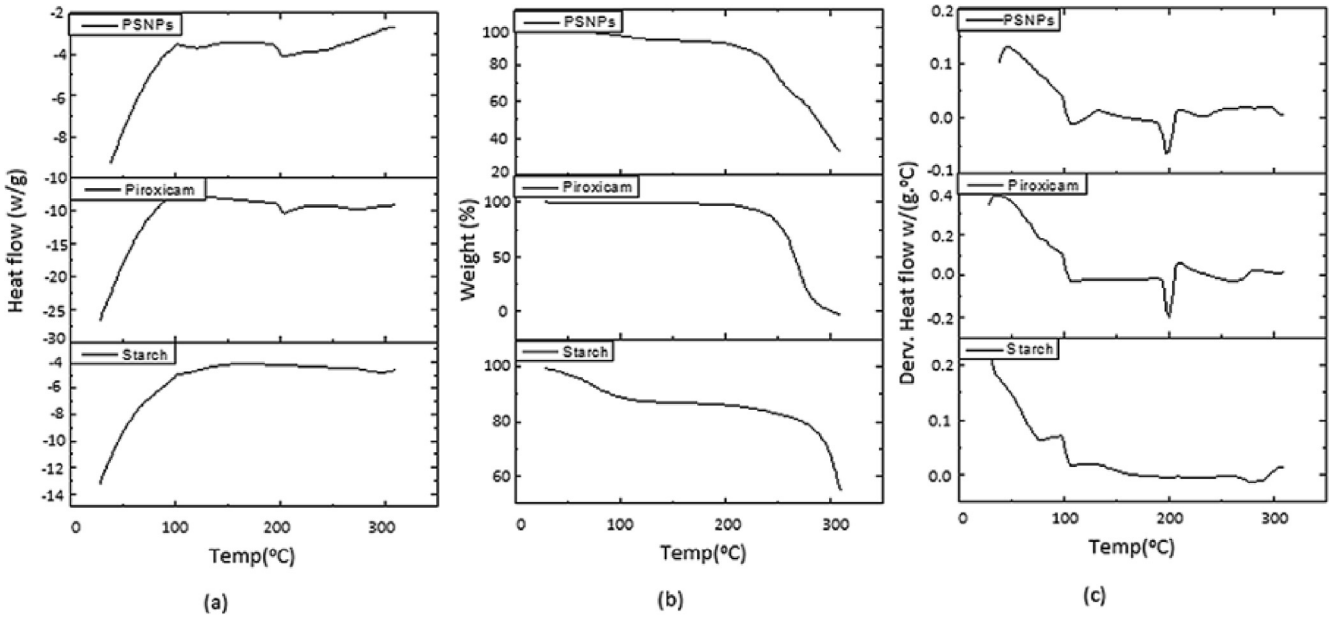

Fig. 2. (a) DSC curves (b) First derivative curves and (c) DTG curves of Starch, Piroxicam and PSNPs.

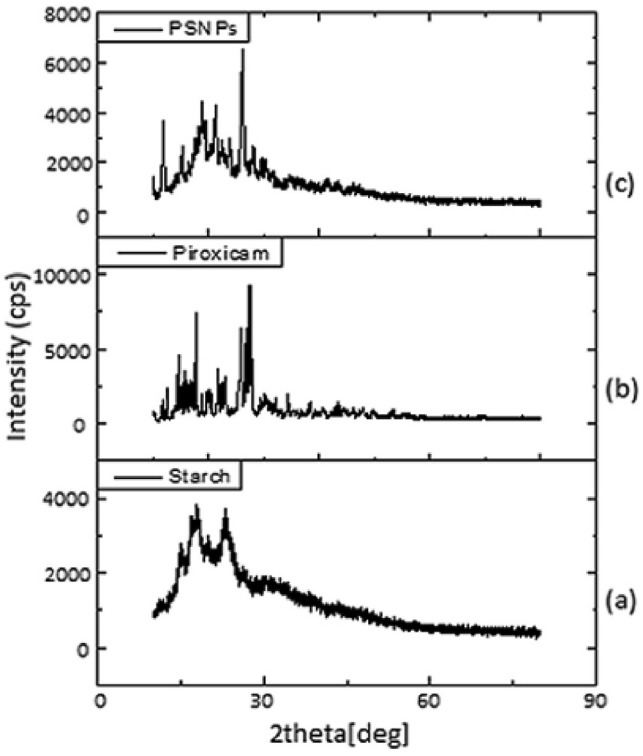

Fig. 3. XRD of (a) Starch (b) Piroxicam (c) PSNPs.

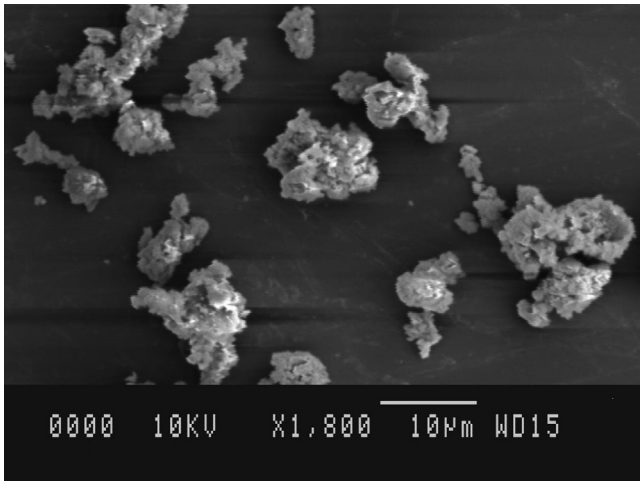

Fig. 4. Surface morphology of PSNPs.

3.5. Experimental design

3.5.1. Particle size analysis

The average particle size and size distribution of piroxicam loaded starch nanoparticles were determined by using zetasizer (Nano ZS90, Malvern Instruments, and UK). During the preliminary trials, it was observed that concentration of starch and piroxicam influence the average particle size and size distribution. Therefore, concentration of starch (X_1) and concentration of piroxicam (X_2) were chosen as the formulation variables for optimization of preparation of PSNPs with the constraints of minimum z-avg. and PdI.

Table 1 displays the results of z-avg. (Y_1) and PdI (Y_2) of the PSNPs prepared, according to the design expert protocol. By utilizing the experimental design the produced responses were fitted into several polynomial models. The responses z-avg (Y_1) and PdI (Y_2) were best fitted into the quadratic response surface model without any transformation of the data.

The polynomial models for the responses z-avg (Y_1) and PdI (Y_2) can also be expressed by the Eqs. (5) and (6), respectively. The positive and negative coefficient value for specific independent variables in the polynomial Eqs. (5) and (6) explains the synergistic and antagonist effects, respectively.

$$(Y_1) = 422.78 - 160.10X_1 + 76.82X_2 - 126.52X_1X_2 + 170.87X_1^2 - 119.38X_2^2 \quad (5)$$

$$(Y_2) = 0.49 - 0.12X_1 + 0.047X_2 - 0.10X_1X_2 + 0.091X_1^2 - 0.084X_2^2 \quad (6)$$

Table 2 summarizes the outcomes of ANOVA test on the response surface quadratic model demonstrating that model was significant with non-significant lack of fit. Further, R^2- value (>0.9) specify a good correlation among experimental and predicted responses. The adequate precision measures signal to noise ratio and a ratio greater than 4 is desirable. In this design, the ratio of 17.412 demonstrated an adequate signal. Therefore, model can be used to navigate design space (see Table 3).

Fig. 5(a) and (b) shows the combined effect of concentration of starch and piroxicam on the z-avg and PdI respectively. It was noticed that lowering the concentration of starch favours the lower particle size, but increased concentration of piroxicam to the formulation increases the particle size i.e. increased loading of piroxcam in the formulation resulted in increased particle size and shows greater influence on the z-avg in the nanoparticle formulations as compared to effect of concentration of quinoa starch, depicted in the Fig. 5(a).

Fig. 5(b) displays the polydispersity index and it is a dimensionless number which displays the degree of uniformity of particles size. Lower PdI values show more uniformity in the particle size whereas higher polydispersity index displays non-uniformity of particle size. The results demonstrated that the effect of piroxicam on PdI is more prominent as compared to quinoa starch (eq^n 6). In different batches of nanoparticles, polydispersity index displayed the range from the 0.339 to 0.772.

The concentration of starch and piroxicam was optimized with the constraints of having PSNPs with minimum average particle size and PdI. An optimization tool in design expert software provided the different sets of solution. The suggested parameters were concentration of starch (9.96 mg/ml) and concentration of piroxicam (9.99 mg/ml) that provided PSNPs of particle size 292.9 nm (predicted 264.32 nm) and PdI 0.479 (predicted 0.322). The predicted and observed values are in the closer agreement that stipulated high prognostic ability of the polynomial model.

3.6. Entrapment efficiency and drug loading

The entrapment efficiency of optimized batch was determined and found to be 78% whereas drug loading of PSNPs was found to be 84%. Hence, it may be said that the drug piroxicam was successfully loaded and entrapped with a good percentage in the starch nanoparticles.

Table 2
Model summary statistics.

Response factors						Lack of fit	
	F-value (%)	Prob. > F	R^2	Adeq. Prec	C.V. (%)	F-value	Prob. > f
Y_1 (Z-avg)	25.73	0.0002	0.9484	17.412	11.57	1.59	0.3247
Y_2 (PdI)	27.73	0.0002	0.9519	18.562	7.08	0.62	0.6405

Table 3
Release kinetics and modeling data of piroxicam solution and PSNPs.

Formulation	Zero Order	First Order	Higuchi	Korsemeyer-Peppas	
	R^2	R^2	R^2	R^2	N
Piroxicam solution	0.968	0.979	0.954	0.945	0.747
PSNPs	0.863	0.599	0.721	0.878	0.906

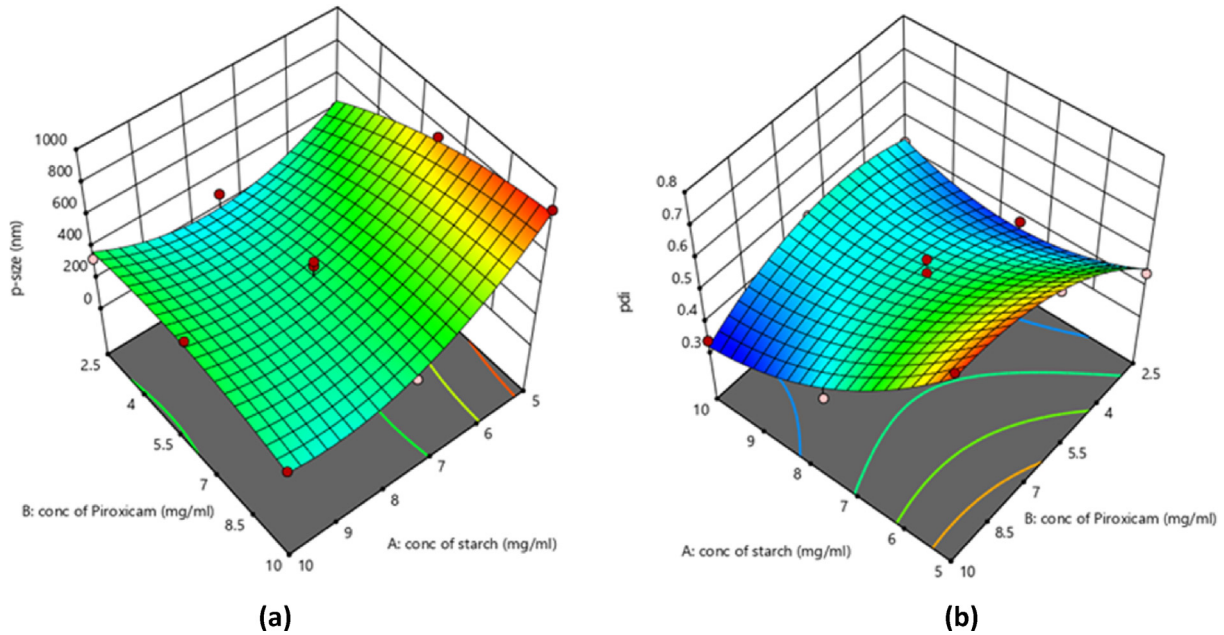

Fig. 5. Effect of concentration of starch and piroxicam on (a) Z-average (b) PdI.

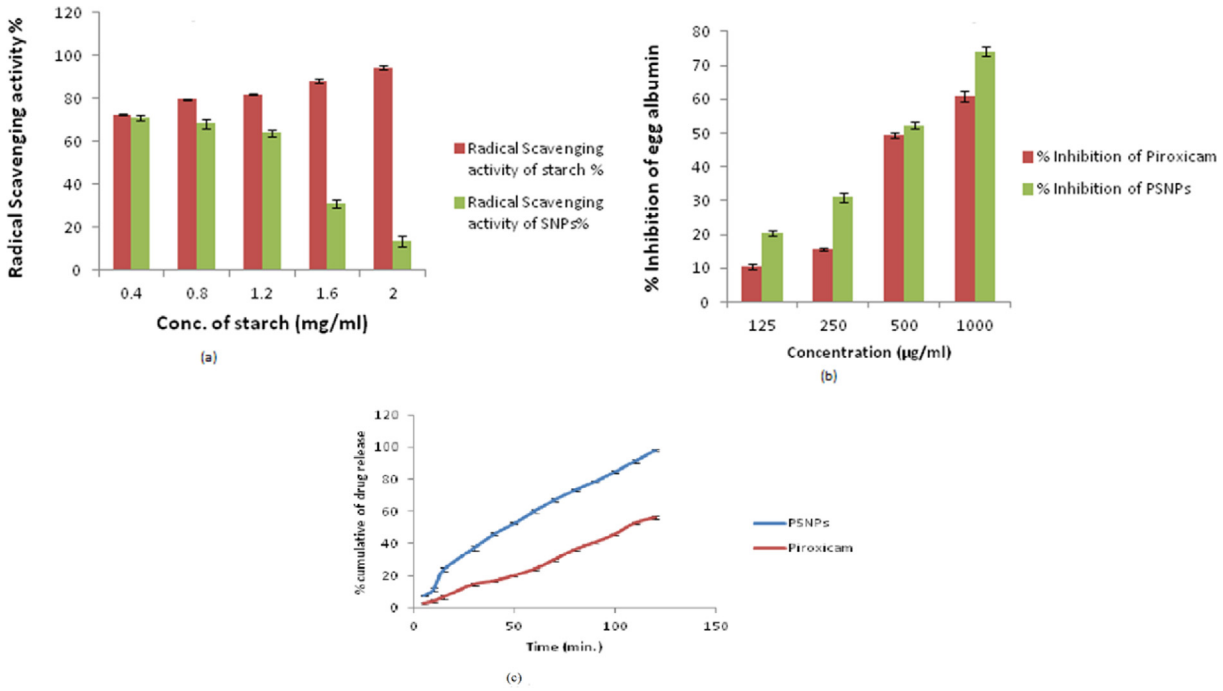

Fig. 6. (a) Percent inhibition of Piroxicam and PSNPs (b) DPPH radical scavenging activity of Starch and SNPs, (c) In-vitro release profile of Piroxicam and PSNPs in 0.1 N HCl.

3.7. DPPH radical scavenging activity

As DPPH radical contains odd electrons due to which the solutions of DPPH radical in the organic solvents gives a deep violet color. They display a strong absorbance at a wavelength of 517 nm. In the existence of antioxidants such as starch, reduction of DPPH radical takes place, odd electron get paired, continuous discoloration is noted and absorption gets disappeared (Farrag et al., 2018; Wen et al., 2016) . Fig. 6 (b) displays the DPPH radical scavenging activity of starch and blank SNPs at varying concentrations (0.4, 0.8 1.2, 1.6 and 2 mg/ml). The results demonstrated that at lower concentration no significant difference between the radical scavenging activity is observed but on higher concentration of starch the DPPH radical scavenging activity of starch is quiet high as compared to SNPs. This drop in radical scavenging activity of SNPs may be due to interference of acid that is used during the preparation of starch nanoparticles. In the presence of acid, amorphous regions are hydrolyzed preferentially that further also enhances the crystallinity. Thus, a decrease in radical scavenging activity was observed (Wang and Copeland, 2015).

3.8. In-vitro anti-inflammatory activity

Fig. 6(a) shows the in-vitro anti-inflammatory activity of the drug piroxicam and PSNPs through the egg albumin denaturation method. The results demonstrated that the % inhibition of formulation PSNPs is much more than the model drug piroxicam. It is observed from the study that increasing concentration of piroxicam in formulation and piroxicam alone shows an increase in anti-inflammatory activity. But on comparing the effect, it is clear that PSNPs is more effective as compared to drug piroxicam in its pure form. Thus, PSNPs renders piroxicam more active because of its fast dissolution than the pure drug piroxicam.

3.9. In-vitro release study

Fig. 6(c) illustrates the in-vitro release study of the piroxicam from the optimized formulation of PSNPs and piroxicam solution in equivalent concentration in the medium of 0.1 N HCl. The release profile of the PSNPs demonstrates the maximum drug release about 98.8% over a specific period of 120 min in the medium as compared to the piroxicam that shows approximately 60% release in 120 min. Thereby, it is inferred that formation of nanoparticles has enhanced the drug release. The *in-vitro* release of piroxicam from the PSNPs and from the piroxicam solution was subjected to the various release kinetics models such as Zero order, First order, Higuchi model and korsemeyer-peppas model etc. In-vitro release rate of drug from PSNPs was best fitted into the Korsemeyer-peppas model with the regression value ($R^2 = 0.878$) with "n" value of 0.906 which indicates the release of piroxicam from the PSNPs occurs through the Super case II transport diffusion mechanism.

4. Conclusion

Quinoa seed starch was extracted through water steeping method. SNPs loaded with model drug piroxicam were prepared to enhance the solubility of drug by using the nanoprecipitation technique. The piroxicam loaded SNPs were optimized by using the 2-factor, 3-level central composite experimental design and then evaluated for particle size and polydispersity index. The particle size range of developed nanoparticles was found to be 282.9–870.5 nm. The DSC studies of the PSNPs demonstrated the increased crystallinity of the product indicating the modification has taken place. TGA-DTA curves of PSNPs showed the thermal stability. Entrapment efficiency and drug loading was found to be 78% and 84%, respectively. SEM shows the flaky, rough and granular surface of the nanoparticles. The DPPH radical scavenging activity of the PSNPs was less as compared to SNPS that may be due to acid interaction during the preparation of formulation while quinoa starch shows good anti oxidant activity. The anti-inflammatory activity carried out using egg albumin denaturation method exhibited that PSNPs displayed high anti-inflammatory activity as compared to pure drug piroxicam indicating that PSNPs are more active than the pure drug whereas in-vitro release profile of piroxicam from the nanoparticles showed the 78% drug release in the 0.1 N

HCl in 2 h. Based on study carried out here, it is inferred from the results and observations that quinoa starch has increased the release rate of drug piroxicam with enhanced anti-inflammatory property whereas the radical scavenging activity was found to be lowered. Therefore quinoa starch possesses the excellent potential as a carrier that can be explored for future applications in the field of pharmaceutical research.

Acknowledgement

The authors acknowledge the facilities provided by DST-PURSE and Guru Jambheshwar University of Science and Technology, Hisar, Haryana (India).

Declaration of Competing Interest

There is no conflict of interest between authors.

References

Adebisi, A.O., Kaialy, W., Hussain, T., Al-Hamidi, H., Nokhodchi, A., Conway, B.R., Asare-Addo, K., 2016. Solid-state, triboelectrostatic and dissolution characteristics of spray-dried piroxicam-glucosamine solid dispersions. Colloids Surf., B 146, 841–851. https://doi.org/10.1016/j.colsurfb.2016.07.032.

Ahmad, M., Mudgil, P., Gani, A., Hamed, F., Masoodi, F.A., Maqsood, S., 2019a. Nano-encapsulation of catechin in starch nanoparticles: characterization, release behavior and bioactivity retention during simulated in-vitro digestion. Food Chem. 270, 95–104.

Ahmad, M., Gani, A., Hamed, F., Maqsood, S., 2019b. Comparative study on utilization of micro and nano sized starch particles for encapsulation of camel milk derived probiotics (Pediococcus acidolactici). LWT 110, 231–238.

Ahmad, M., Gani, A., Hassan, I., Huang, Q., Shabbir, H., 2020. Production and characterization of starch nanoparticles by mild alkali hydrolysis and ultra-sonication process. Sci. Rep. 10 (1), 1–11.

Ahmad, M., Gani, A., Masoodi, F.A., Rizvi, S.H., 2020. Influence of ball milling on the production of starch nanoparticles and its effect on structural, thermal and functional properties. Int. J. Biol. Macromol. 151, 85–91.

Ahuja, M., Bhatia, M., Saini, K., 2016. Sodium alginate–arabinoxylan composite microbeads: preparation and characterization. J. Pharm. Invest. 46 (7), 645–653. https://doi.org/10.1007/s40005-016-0244-1.

Ali, H.S., York, P., Blagden, N., 2009. Preparation of hydrocortisone nanosuspension through a bottom-up nanoprecipitation technique using microfluidic reactors. Int. J. Pharm. 375 (1–2), 107–113. https://doi.org/10.1016/j.ijpharm.2009.03.029.

Angellier, H., Choisnard, L., Molina-Boisseau, S., Ozil, P., Dufresne, A., 2004. Optimization of the preparation of aqueous suspensions of waxy maize starch nanocrystals using a response surface methodology. Biomacromolecules 5 (4), 1545–1551. https://doi.org/10.1021/bm049914u.

Araújo, A., Galvão, A., Silva Filho, C., Mendes, F., Oliveira, M., Barbosa, F., Bastos, M., 2018. Okra mucilage and corn starch bio-based film to be applied in food. Polym. Test. 7, 352–361. https://doi.org/10.1016/j.polymertesting.2018.09.010.

Bhatia, M., Ahuja, M., 2013. Thiol modification of psyllium husk mucilage and evaluation of its mucoadhesive applications. Sci. World J. https://doi.org/10.1155/2013/284182.

Bhatia, M., Ahuja, M., Mehta, H., 2015. Thiol derivatization of Xanthan gum and its evaluation as a mucoadhesive polymer. Carbohydr. Polym. 131, 119–124. https://doi.org/10.1016/j.carbpol.2015.05.049.

Bhatia, M., Saini, M., 2018. Formulation and evaluation of curcumin microsponges for oral and topical drug delivery. Prog. Biomater. 7 (3), 239–248. https://doi.org/10.1007/s40204-018-0099-9.

Bramosanti, M., Chronopoulou, L., Grillo, F., Valletta, A., Palocci, C., 2017. Microfluidic-assisted nanoprecipitation of antiviral-loaded polymeric nanoparticles. Colloids Surf., A 532, 369–376. https://doi.org/10.1016/j.colsurfa.2017.04.062.

Chan, S.Y., Goh, C.F., Lau, J.Y., Tiew, Y.C., Balakrishnan, T., 2019. Rice starch thin films as a potential buccal delivery system: effect of plasticiser and drug loading on drug release profile. Int. J. Pharm. 562, 203–211. https://doi.org/10.1016/j.ijpharm.2019.03.044.

Chavan, R.R., Hosamani, K.M., 2018. Microwave-assisted synthesis, computational studies and antibacterial/anti-inflammatory activities of compounds based on coumarin-pyrazole hybrid. R. Soc. Open Sci. 5, (5). https://doi.org/10.1098/rsos.172435 172435.

D'Amico, S., Jungkunz, S., Balasz, G., Foeste, M., Jekle, M., Tömösköszi, S., Schoenlechner, R., 2019. Abrasive milling of quinoa: study on the distribution of selected nutrients and proteins within the quinoa seed kernel. J. Cereal Sci. 86, 132–138. https://doi.org/10.1016/j.jcs.2019.01.007.

Devi, R., Bhatia, M., 2019. Thiol functionalization of flaxseed mucilage: preparation, characterization and evaluation as mucoadhesive polymer. Int. J. Biol. Macromol. 126, 101–106. https://doi.org/10.1016/j.ijbiomac.2018.12.116.

Ding, S., Serra, C.A., Anton, N., Yu, W., Vandamme, T.F., 2019. Production of dry-state ketoprofen-encapsulated PMMA NPs by coupling micromixer-assisted nanoprecipitation and spray drying. Int. J. Pharm. 558, 1–8. https://doi.org/10.1016/j.ijpharm.2018.12.031.

El-Sheikh, M.A., 2017. New technique in starch nanoparticles synthesis. Carbohydr. Polym. 176, 214–219. https://doi.org/10.1016/j.carbpol.2017.08.033.

Farrag, Y., Ide, W., Montero, B., Rico, M., Rodríguez-Llamazares, S., Barral, L., Bouza, R., 2018. Preparation of starch nanoparticles loaded with quercetin using nanoprecipitation technique. Int. J. Biol. Macromol. 114, 426–433. https://doi.org/10.1016/j.ijbiomac.2018.03.134.

Fu, Z., Li, L., Wang, Y., Chen, Q., Zhao, F., Dai, L., Guo, X., 2019. Direct preparation of drug-loaded mesoporous silica nanoparticles by sequential flash nanoprecipitation. Chem. Eng. J. 122905. https://doi.org/10.1016/j.cej.2019.122905.

Gandhi, A., Jana, S., Sen, K.K., 2014. In-vitro release of acyclovir loaded Eudragit RLPO® nanoparticles for sustained drug delivery. Int. J. Biol. Macromol. 67, 478–482. https://doi.org/10.1016/j.ijbiomac.2014.04.019.

Gholivand, M.B., Malekzadeh, G., Derakhshan, A.A., 2014. Boehmite nanoparticle modified carbon paste electrode for determination of piroxicam. Sens. Actuators, B 201, 378–386. https://doi.org/10.1016/j.snb.2014.04.054.

Gopi, S., Amalraj, A., Jude, S., Thomas, S., Guo, Q., 2019. Bionanocomposite films based on potato, tapioca starch and chitosan reinforced with cellulose nanofiber isolated from turmeric spent. J. Taiwan Inst. Chem. Eng. 96, 664–671. https://doi.org/10.1016/j.jtice.2019.01.003.

Govender, T., Stolnik, S., Garnett, M.C., Illum, L., Davis, S.S., 1999. PLGA nanoparticles prepared by nanoprecipitation: drug loading and release studies of a water soluble drug. J. Control. Release 57 (2), 171–185. https://doi.org/10.1016/S0168-3659(98)00116-3.

Jan, K.N., Panesar, P.S., Singh, S., 2017. Process standardization for isolation of quinoa starch and its characterization in comparison with other starches. J. Food Meas. Charact. 11 (4), 1919–1927. https://doi.org/10.1007/s11694-017-9574-6.

Khan, W.H., Rathod, V.K., 2014. Process intensification approach for preparation of curcumin nanoparticles via solvent–nonsolvent nanoprecipitation using spinning disc reactor. Chem. Eng. Process. Process Intensif. 80, 1–10. https://doi.org/10.1016/j.cep.2014.03.011.

Legrand, E., 2004. Aceclofenac in the management of inflammatory pain. Expert Opin. Pharmacother. 5 (6), 1347–1357. https://doi.org/10.1517/14656566.5.6.1347.

Letelier, M.E., Rodríguez-Rojas, C., Sánchez-Jofré, S., Aracena-Parks, P., 2011. Surfactant and antioxidant properties of an extract from Chenopodium quinoa Willd seed coats. J. Cereal Sci. 53 (2), 239–243. https://doi.org/10.1016/j.jcs.2010.12.006.

Liu, C.S., Desai, K.G.H., Meng, X.H., Chen, X.G., 2007. Sweet potato starch microparticles as controlled drug release carriers: preparation and in vitro drug release. Drying Technol. 25 (4), 689–693. https://doi.org/10.1080/07373930701290977.

Liu, Q., Li, M., Xiong, L., Qiu, L., Bian, X., Sun, C., Sun, Q., 2018. Oxidation modification of debranched starch for the preparation of starch nanoparticles with calcium ions. Food Hydrocolloids 85, 86–92. https://doi.org/10.1016/j.foodhyd.2018.07.004.

Papadimitriou, S., Bikiaris, D., 2009. Novel self-assembled core–shell nanoparticles based on crystalline amorphous moieties of aliphatic copolyesters for efficient controlled drug release. J. Control. Release 138 (2), 177–184. https://doi.org/10.1016/j.jconrel.2009.05.013.

Qin, Y., Liu, C., Jiang, S., Xiong, L., Sun, Q., 2016. Characterization of starch nanoparticles prepared by nanoprecipitation: influence of amylose content and starch type. Ind. Crops Prod. 87, 182–190. https://doi.org/10.1016/j.indcrop.2016.04.038.

Rayner, M., Sjöö, M., Timgren, A., Dejmek, P., 2012. Quinoa starch granules as stabilizing particles for production of Pickering emulsions. Faraday Discuss. 158 (1), 139–155. https://doi.org/10.1039/C2FD20038D.

Rivas, C.J.M., Tarhini, M., Badri, W., Miladi, K., Greige-Gerges, H., Nazari, Q.A., Elaissari, A., 2017. Nanoprecipitation process: From encapsulation to drug delivery. Int. J. Pharm. 532 (1), 66–81. https://doi.org/10.1016/j.ijpharm.2017.08.064.

Sezgin, A.C., Sanlier, N.A., 2019. New generation plant for the conventional cuisine: quinoa (chenopodium quinoa willd.). Trends Food Sci. Technol. https://doi.org/10.1016/j.tifs.2019.02.039.

Stikic, R., Glamoclija, D., Demin, M., Vucelic-Radovic, B., Jovanovic, Z., Milojkovic-Opsenica, D., Milovanovic, M., 2012. Agronomical and nutritional evaluation of quinoa seeds (Chenopodium quinoa Willd.) as an ingredient in bread formulations. J. Cereal Sci. 55 (2), 132–138. https://doi.org/10.1016/j.jcs.2011.10.010.

Ubeyitogullari, A., Ciftci, O.N., 2016. Formation of nanoporous aerogels from wheat starch. Carbohydr. Polym. 147, 125–132. https://doi.org/10.1016/j.carbpol.2016.03.086.

Wang, S., Copeland, L., 2015. Effect of acid hydrolysis on starch structure and functionality: a review. Crit. Rev. Food Sci. Nutr. 55 (8), 081–1097. https://doi.org/10.1080/10408398.2012.684551.

Wang, Y., Tan, Y., 2016. Enhanced drug loading capacity of 10-hydroxycamptothecin-loaded nanoparticles prepared by two-step nanoprecipitation method. J. Drug Delivery Sci. Technol. 36, 183–191. https://doi.org/10.1016/j.jddst.2016.09.012.

Wen, Y., Ye, F., Zhu, J., Zhao, G., 2016. Corn starch ferulates with antioxidant properties prepared by N, N′-carbonyldiimidazole-mediated grafting procedure. Food Chem. 208, 1–9. https://doi.org/10.1016/j.foodchem.2016.03.094.

Xu, G.Y., Liao, A.M., Huang, J.H., Zhang, J.G., Thakur, K., Wei, Z.J., 2019. Evaluation of structural, functional, and anti-oxidant potential of differentially extracted polysaccharides from potatoes peels. Int. J. Biol. Macromol. 129, 778–785. https://doi.org/10.1016/j.ijbiomac.2019.02.074.

Zhang, J.Y., Shen, Z.G., Zhong, J., Hu, T.T., Chen, J.F., Ma, Z.Q., Yun, J., 2006. Preparation of amorphous cefuroxime axetil nanoparticles by controlled nanoprecipitation method without surfactants. Int. J. Pharm. 323 (1–2), 153–160. https://doi.org/10.1016/j.ijpharm.2006.05.048.